



# Single-Cell Analysis, Spatial Transcriptomics and Molecular Docking Unveil Potential Therapeutic Targets for Carotid Atherosclerosis

Rongxing Qin<sup>1#</sup>, Hongyu Xu<sup>2#</sup>, Qingchun Qin<sup>1,3</sup>, Wei Xu<sup>1,3</sup>, Xinyu Lai<sup>1</sup>, Li Chen<sup>1,3</sup>

<sup>1</sup>Department of Neurology, The First Affiliated Hospital of Guangxi Medical University, Nanning, Guangxi Zhuang Autonomous Region, China

<sup>2</sup>Department of Neurology, Affiliated Minzu Hospital of Guangxi Medical University, Nanning, China

<sup>3</sup>National Center for International Biotargeting Theranostics, Guangxi Key Laboratory of Biotargeting Theranostics, Collaborative Innovation Center for Targeting Tumor Theranostics, Guangxi Medical University, Nanning, China

#These authors contributed equally to this work

**Background:** Carotid atherosclerosis (CAS) is a key cause of ischemic stroke that is strongly associated with increased risks of cardiovascular disease and vascular death, hence the urgent need to develop therapeutic strategies targeting carotid atherosclerotic plaques that would reduce the overall risk of cerebrovascular events.

**Aims:** This study performs single-cell sequencing to dissect the cellular subpopulations in CAS. Molecular docking is used to uncover the potential therapeutic targets, consequently providing a theoretical basis for the CAS treatment strategies.

**Study Design:** Integrated single-cell, spatial transcriptomic and molecular docking analysis.

**Methods:** The single-cell sequencing data were retrieved from the Gene Expression Omnibus. Enrichment analyses were performed to characterize the cellular subpopulation functions. Accordingly, cell-cell communication networks were mapped to uncover the inter-subgroup

interactions. Molecular docking was also employed to identify the potential therapeutic targets.

**Results:** In this study, we identified the multiple cellular subpopulations that are associated with CAS. These CAS-related subpopulations engage in intercellular communication via distinct signaling pathways. Cannabidiol exhibits strong binding affinities for the macrophage, endothelial, and vascular smooth muscle cell markers. Spatial transcriptomics revealed that *ACTC1*, *AKR1C2*, and *FABP4* exhibit region-specific expression patterns within the plaque.

**Conclusion:** Dissecting the diverse cellular subpopulations in CAS and elucidating their functions and mechanisms, this study integrates single-cell sequencing, molecular docking, and spatial transcriptomics to offer fresh insights into CAS therapy.

## INTRODUCTION

Carotid atherosclerosis is a key cause of ischemic stroke. According to the global epidemiological data, 13-31% of adults have carotid artery plaques, among which those with moderate to severe stenosis account for approximately 2-4%.<sup>1,2</sup> Carotid atherosclerosis is a systemic atherosclerosis manifestation that markedly increases the risk of cardiovascular events and vascular death.<sup>3-5</sup> The carotid artery

plaque measurement is widely performed, as it can quantify the degree of atherosclerosis, assess the risk of future stroke, and serve as a surrogate endpoint for clinical diseases.<sup>6</sup> Carotid artery plaques have a higher predictive value for vascular events, with the risk of vascular events in individuals with carotid artery plaques being 2.8 times compared to that of those without.<sup>7,8</sup> Therefore, the early prevention and intervention of carotid atherosclerosis are greatly significant for reducing the overall cerebrovascular risk.



**Corresponding author:** Li Chen, Department of Neurology, The First Affiliated Hospital of Guangxi Medical University, Nanning, Guangxi Zhuang Autonomous Region, China; National Center for International Biotargeting Theranostics, Guangxi Key Laboratory of Biotargeting Theranostics, Collaborative Innovation Center for Targeting Tumor Theranostics, Guangxi Medical University, Nanning, China

**e-mail:** chenli@gxmu.edu.cn

**Received:** August 16, 2025 **Accepted:** October 16, 2025 **Available Online Date:** xxxxxx • **DOI:** 10.4274/balkanmedj.galenos.2025.2025-8-151

Available at [www.balkanmedicaljournal.org](http://www.balkanmedicaljournal.org)

**ORCID iDs of the authors:** R.Q. 0000-0002-4447-6575; H.X. 0009-0002-0057-9465; Q.Q. 0000-0003-1282-9070; W.X. 0000-0001-8062-7986; X.L. 0000-0001-6906-9725; L.C. 0000-0002-9478-6432.

**Cite this article as:** Qin R, Xu H, Qin Q, Xu W, Lai X, Chen L. Single-Cell Analysis, Spatial Transcriptomics and Molecular Docking Unveil Potential Therapeutic Targets for Carotid Atherosclerosis. *Balkan Med J*;

Copyright@Author(s) - Available online at <http://balkanmedicaljournal.org/>

The single-cell RNA sequencing (scRNA-seq) has now evolved into an important technical tool for exploring cellular heterogeneity, intercellular crosstalk, and transcriptomic dynamic characteristics during the disease progression stage.<sup>9</sup> The application of the scRNA-seq technology in atherosclerosis research is increasingly widespread, with the single-cell atlases of atherosclerotic plaques and circulating blood being previously constructed.<sup>10,11</sup> The increase in the number of macrophages within the plaque is closely associated with the increased plaque instability and lesion progression.<sup>12</sup> Given that plaque cells [i.e., smooth muscle cells, endothelial cells (ECs), and macrophages] exist in a transitional state, exhibit high dynamicity, and can alter their phenotypes in the active plaque microenvironment, changes in the cell states may possibly be determined by changes in intercellular communication.<sup>13–16</sup> Despite the certain progress made in previous studies, the regulatory mechanisms, interactions, and roles of various cells involved in carotid atherosclerosis (CAS) occurrence and development have not yet been fully elucidated to date.

The development of drugs targeting CAS remains a top priority. Cannabidiol (CBD) is a natural extract derived from *Cannabis sativa* that possesses antioxidant and anti-inflammatory properties and serves as a therapeutic agent for atherosclerosis.<sup>17</sup> CBD can alleviate inflammatory responses and barrier disruption in ECs, thereby exhibiting therapeutic potential for atherosclerosis.<sup>18</sup> Studies show that CBD can act as a candidate drug for treating atherosclerosis by activating PPAR $\gamma$  and upregulating the *ABCA1/ABCG1* expression.<sup>19</sup> However, the current characteristics of the interactions between CBD and different cell types in CAS and those between CBD and key cellular molecules remain unknown.

This study utilizes scRNA-seq to explore the key cell populations in CAS and further deepen the understanding of the molecular regulatory mechanisms of CAS. This work applies the CellChat analysis to construct a ligand-receptor interaction network between cells. The binding characteristics of CBD with the specific marker genes of the contractile muscle cells (MCs), ECs, and vascular smooth MCs (VSMCs) are initially screened out through molecular docking. The binding targets of CBD in different cells are then identified. This research provides a certain theoretical basis for developing CAS treatment strategies.

## MATERIALS AND METHODS

### Single-cell transcriptome analysis

We analyzed the scRNA-seq dataset of human carotid plaques (GSE159677). It comprises three AC samples and patient-matched peripheral artery (PA) portions. We performed quality control using Seurat (v4.3.1). The criteria for filtering out the low-quality cells were detected genes fewer than 500 or more than 2,500 or a mitochondrial gene proportion higher than 5%. The R package DoubletFinder was used to predict and remove the doublets. A total of 26,392 cells were retained after the abovementioned analysis was performed.

We corrected the batch effects using Harmony. The data processing workflow included normalization, principal component analysis (PCA) dimensionality reduction based on the top 30 principal components, uniform manifold approximation and projection (UMAP) visualization, and unsupervised clustering using the FindClusters function (resolution = 0.2). The marker genes for each clustered subgroup were identified using the FindAllMarkers function. Each subgroup was subsequently annotated. The cell clusters were identified as specific cell types and presented in Supplementary Table 1.

### Functional enrichment analysis

The differential expression genes were subjected to a gene ontology (GO) and Kyoto Encyclopedia of Genes and Genomes (KEGG) pathway enrichment analysis using the clusterProfiler package.<sup>20</sup> The significance threshold was set at false discovery rate (FDR) < 0.05.

### Cell communication network construction

CellChat (v1.1.0) was applied to parse the interactions between cells covering the ligand-receptor-cofactor interaction networks. The average gene expression of each cell cluster was aggregated to calculate the interaction probability of the ligand-receptor pairs. The significance was determined at  $p < 0.05$ .

### VECTOR

VECTOR can be used to infer the developmental direction vectors of the cells in UMAP. It treats the two-dimensional UMAP cell representation as an image and divides it into multiple pixel units. After removing the pixels that do not contain any cells, VECTOR then focuses on the largest connected pixel network in UMAP to achieve the inference of the cell developmental directions.<sup>21</sup>

### Molecular docking

The target protein crystal structures were obtained from the Research Collaboratory for Structural Bioinformatics Protein Data Bank. Accordingly, molecular docking was performed against the following structures: *CD1E* (PDB ID: 3S6C), *FABP4* (9MIW), *KLRB1* (5MGR), *S100A12* (2WCB), *AKR1C2* (2HDJ), *ITLN1* (4WMQ), *DLGAP5* (8X9P), and *CCR7* (6QZH). Molecular docking between the abovementioned protein crystal structures and CBD (CID: 644019) was conducted using the CB-Dock2 online platform (<http://clab.labshare.cn:10380/cb-dock2/>). The AutoDock Vina algorithm was used to evaluate the binding energy (kcal/mol) and the molecular interaction patterns under default parameters. CB-Dock2 offers two docking modes. The first mode involves sequence alignment and pocket prediction with known crystal structures in the PDB database, followed by the molecular docking calculations that are based on the corresponding pockets. The second mode performs the docking simulations on the entire protein receptor and explores the optimal binding mode based on the Vina docking algorithm.

### Spatial transcriptomics processing

The spatial transcriptomic data of the carotid plaque tissue were used in this study. The data were obtained from the GEO database with accession numbers GSE241346 (platform: GPL30173) and sample GSM7727540. The data preprocessing was performed using Seurat (v5.0.1), starting with a strict quality control to remove the low-quality spots with UMI counts < 1,500 or detected gene numbers < 500. The SCTransform method was then used to correct the technical variations for the data normalization. The PCA dimensionality reduction was based on 30 principal components. Spatial clustering maps were constructed using the FindNeighbors and FindClusters functions, with the gene expression patterns being spatially visualized using SpatialFeaturePlot.

### Statistical analysis

All bioinformatics analyses used in this study were conducted using R (v4.3.1). All statistical tests were two-tailed. The enrichment analyses were considered significant at FDR < 0.05 (BH-adjusted), CellChat analyses at uncorrected  $p < 0.05$ , and all two-group comparisons at the Bonferroni-corrected  $p < 0.05$ .

## RESULTS

### Single-cell landscape of CAS

The scRNA-seq data were sourced from the GEO database comprising three samples of the AC plaques and the corresponding PA control samples of the carotid artery tissue. This study utilized cell marker-related databases like the Panglao database, along with the established classical markers from previous research, as the references.<sup>22</sup> Following the quality control and filtering procedures, an integrated analysis was conducted on a total of 26,392 cells, resulting in the identification of 14 cell clusters and six distinct cell types (Figure 1a), including T cells, MCs, ECs, VSMCs, and B and NK T cells (Figure 1b). The top two marker genes are displayed for each cell type in Figure 1c. A comparative analysis revealed that the proportion of the various cell types in the AC group was increased compared to the PA group, as shown in Figure 1d.

### Role of the macrophages in CAS

The cluster analysis of the macrophages identified eight distinct cell subgroups, with the specific genes expressed in these subgroups serving as the specific marker genes, including *IGSF21*, *FABP4*, and *S100A12* (Figures 2a and 2b). The VECTOR analysis of the MC subgroups showed that the *IGSF21*+ MC subgroup depicted the highest differentiation potential, likely representing the developmental origin of the MCs and indicating high differentiation potential and plasticity (Figure 2c). The cell abundance of the *CCDC141*+ MC subgroup in the AC group significantly decreased, while that of the *IGSF21*+ MC, *FABP4*+ MC, *S100A12*+ MC, *CD1E*+ MC, *KLRB1*+ MC, *SHD*+ MC, and *PPY*+ MC subgroups significantly increased, as displayed in Figure 2d. The enrichment analysis revealed the different functional characteristics of these subgroups.

The GO enrichment analysis showed that the *IGSF21*+ MC subgroup was significantly enriched in terms of the MHC class II protein complex assembly and the positive regulation of the cytokine production pathways ( $p < 0.05$ ), indicating its potential role in the immune responses. Figure 3a shows that the *FABP4*+ MC subgroup was significantly enriched in the glycolytic process pathway ( $p < 0.05$ ). The KEGG enrichment analysis revealed that the *CD1E*+ MC subgroup was enriched in the cell adhesion molecules. The *KLRB1*+ MC subgroup was enriched in the T cell receptor signaling pathway (Figure 3b). The CellChat analysis of inter-subgroup communication showed that *CD1E*+ MC communicated with *SHD*+ MC and *CCDC141*+ MC via the GAS signaling pathway (Figure 3c). The communication between the *CD1E*+ MC and *FABP4*+ MC subgroups occurred through the MIF signaling pathway (Figure 3d).

### Role of EC in CAS

A cluster analysis of the EC population revealed a successful identification of six distinct cell subgroups (Figure 4a) characterized by their specific marker genes, namely, *SCARB1*, *IGHA1*, *ITLN1*, *AKR1C2*, *CD3G*, and *DLX4* (Figure 4b). Compared to that of the control group, the cell abundance of the *IGHA1*+ EC and *AKR1C2*+ EC subgroups significantly decreased in the AC group (Figure 4c). The VECTOR analysis of the EC subgroups revealed that the *ITLN1*+ EC subgroup possessed the highest differentiation potential, which may indicate the developmental origin of the EC cells and suggests that this subgroup has high differentiation potential and plasticity (Figure 4d).

The GO enrichment analysis results indicated that the *SCARB1*+ EC subgroup was significantly enriched in the pathways of "taxis" and "chemotaxis" ( $p < 0.05$ ). The *CD3G*+ EC subgroup was significantly enriched in the pathways of "extracellular matrix organization," "EC differentiation," and "antigen receptor-mediated signaling pathway" (Figure 5a). The CellChat analysis of communication between EC subgroups also showed that *AKR1C2*+ EC and *SCARB1*+ EC communicate via the CXCL signaling pathway (Figure 5b), while communication between the *DLX4*+ EC subgroup and the other subgroups occurred through the PTN signaling pathway (Figure 5c).

### Role of VSMC in CAS

A clustering analysis on the VSMC population revealed a successful identification of nine distinct cell subgroups characterized by their specific marker genes, that is, *TFPI2*, *CCL19*, *PART1*, *TSPAN13*, *COX4I2*, *ACTC1*, *FAM180B*, *CCR7*, and *DLGAP5* (Figures 6a and 6b). Compared to that of the control group, the cell abundance of the *COX4I2*+ and *FAM180B*+ VSMC subgroups was significantly reduced in the AC group (Figure 6c). The VECTOR analysis indicated that the *TFPI2*+ VSMC subgroup possessed the highest differentiation potential, possibly suggesting the developmental origin of the VSMCs and indicating that this subgroup has high differentiation potential and plasticity (Figure 6d).

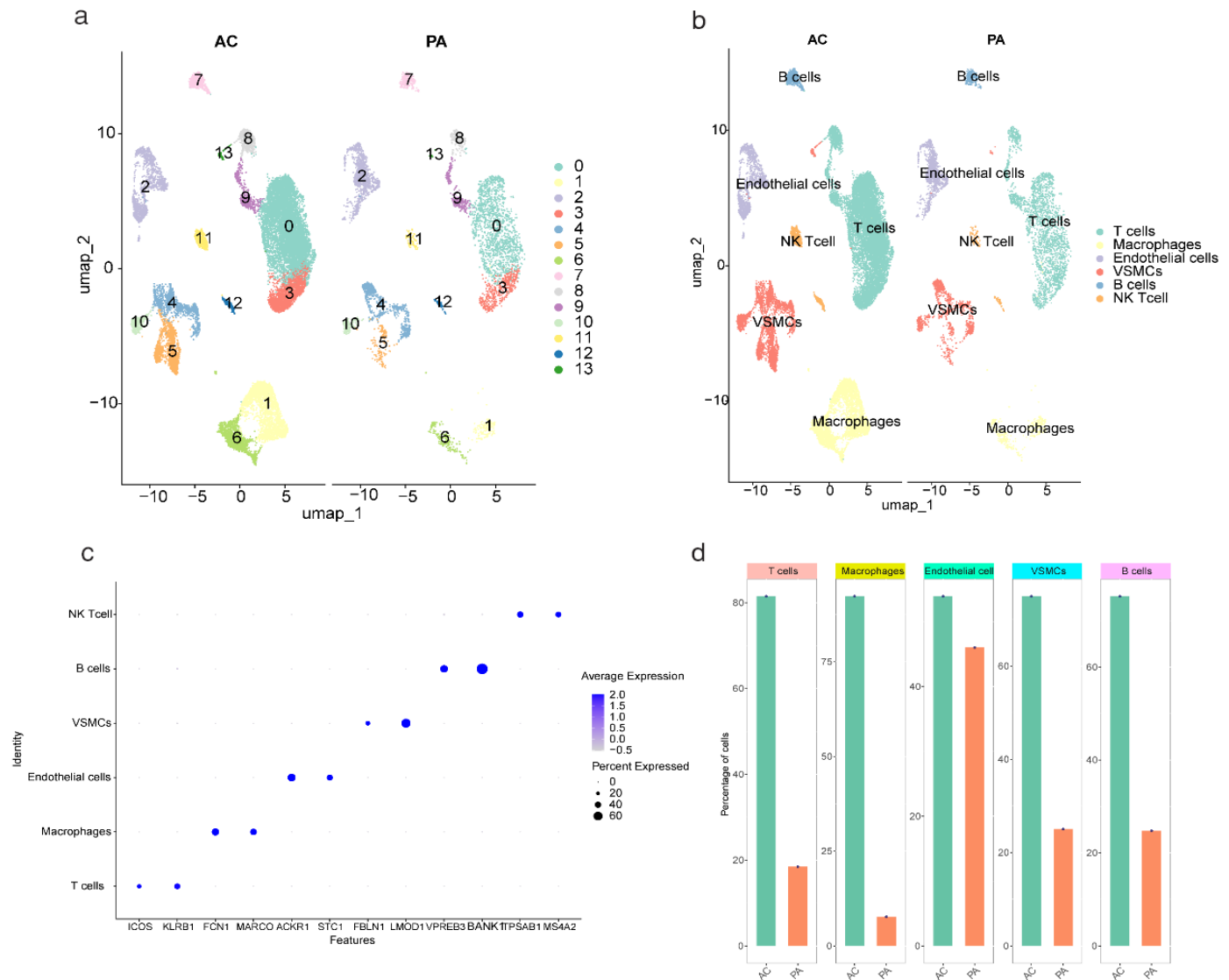


**FIG. 1.** Identification of major cell types in carotid atherosclerotic plaque from atherosclerotic core (AC) and proximal artery (PA) tissues. (a) Uniform manifold approximation and projection (UMAP) plot of all single cells from AC tissues (n = 3 samples) and PA tissues (n = 3 samples), colored by unsupervised clustering. (b) UMAP plot displaying 6 annotated cell types in carotid atherosclerotic plaques from AC and PA tissues. (c) The bubble plot highlights the marker genes specifically expressed in each cell type. (d) Differences in cell counts among different cell types.

VSMCs, vascular smooth muscle cells.

The GO enrichment analysis results revealed that the *FAM180B*+ VSMC subgroup was significantly enriched in the “BMP signaling pathway” ( $p < 0.05$ ). Additionally, the *CCR7*+ and *DLGAP5*+ VSMC subgroups were significantly enriched in the T cell receptor signaling pathway. Moreover, the *CCL19*+ VSMC subgroup was significantly enriched in the pathways related to the muscle system processes, muscle contraction, myofibril assembly, and striated muscle cell development (Figure 7a). The *TFPI2*+ VSMC subgroup was primarily enriched in the “cytoskeleton in muscle cells” and the “protein digestion and absorption” pathways, while the *PART1*+ VSMC

subgroup was primarily enriched in the “vascular smooth muscle contraction” pathway (Figure 7b).

Furthermore, the analysis of the intercellular communication among the VSMC subgroups using CellChat revealed that the *DLGAP5*+ and *CCL19*+ VSMC subgroups and the *FAM180B*+ VSMC subgroups communicated via the TNF signaling pathway (Figure 7c), while the communication between the *CCL19*+ VSMC and *FAM180B*+ VSMC subgroups and the *CCR7*+ VSMC subgroups occurred through the CCL signaling pathway (Figure 7d).

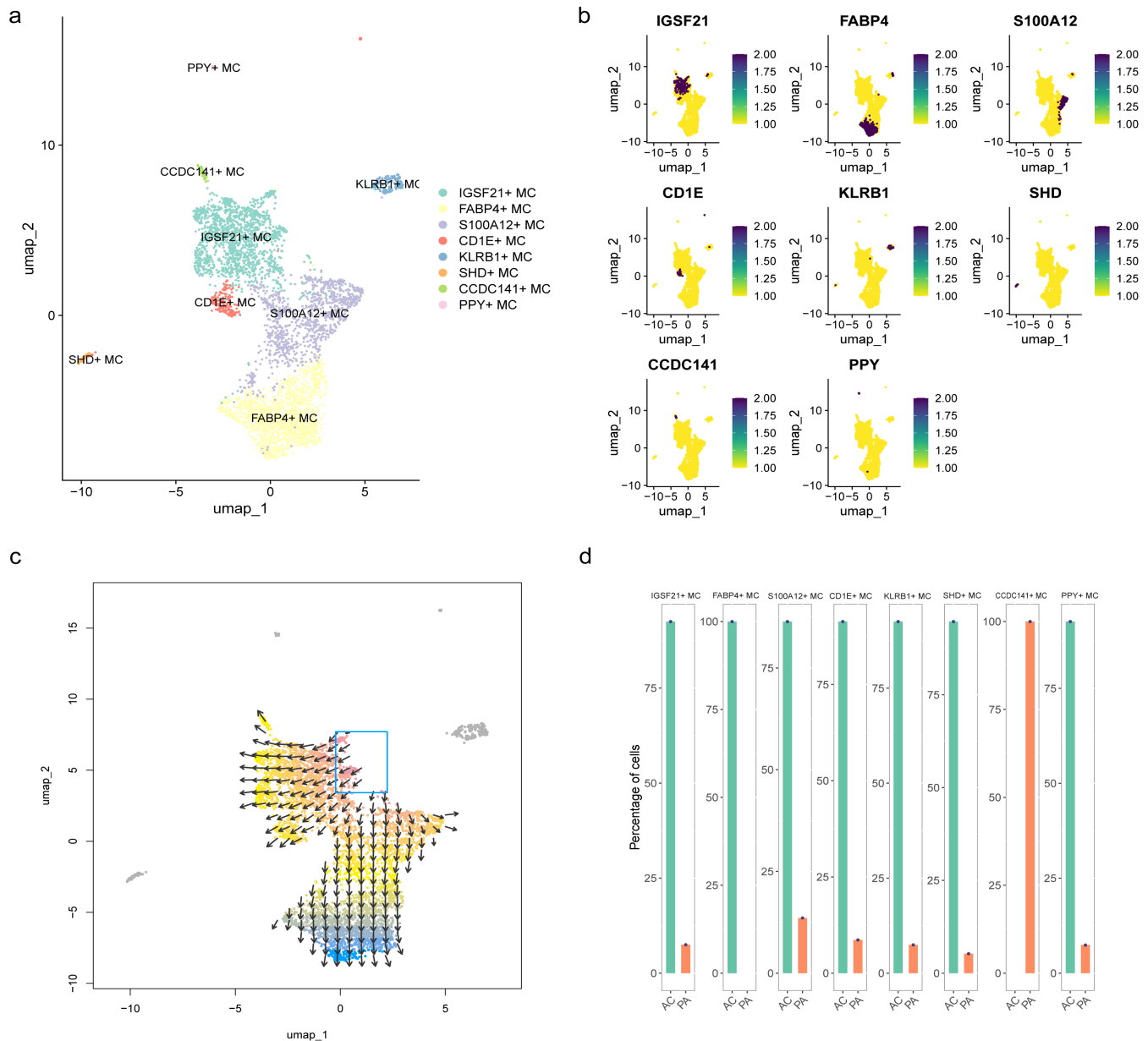


**FIG. 2.** Single-cell transcriptome analysis of macrophage (MCs). (a) The UMAP plot illustrates the distribution of MCs subpopulations, with distinct colors representing different MCs subpopulations. (b) The density map illustrates the spatial density distribution of genes within MCs subpopulations. The purple areas indicate higher cell density, while the yellow areas indicate lower cell density. (c) The VECTOR tool is used to infer the developmental direction of MCs subpopulations. (d) The bar chart illustrates the changes in the abundance of MCs subpopulations between the atherosclerotic core (AC) group and the proximal artery (PA) group.

UMAP, uniform manifold approximation and projection.

### Molecular docking of CBD with the marker genes of different cell types

CBD exerts its effects through immune modulation, thereby significantly altering the immune system's response and delaying the progression of atherosclerosis induced by high glucose levels.<sup>23</sup> The potential interactions between CBD and the marker genes

of different cell types were systematically evaluated by using the developed molecular docking model that targeted the marker genes of the distinct subpopulations of the MCs, ECs, and VSMCs. The potential interactions between CBD and the marker genes of different cell types were evaluated through molecular docking analyses on the marker genes of the distinct subsets of the MCs, ECs, and VSMCs.



The free binding energies of CBD with *CD1E*, *FABP4*, *KLRB1*, and *S100A12* in the MCs were calculated as -8.1, -6.1, -6.7, and -6.8 kcal/mol, respectively (Figures 8a-d), while those in the ECs of CBD with *AKR1C2* and *ITLN1* were -8.8 and -5.6 kcal/mol, respectively (Figures 9a and 9b). In the VSMCs, the free binding energies of CBD with *DLGAP5* and *CCR7* were -7.0 and -7.4 kcal/mol, respectively (Figures 10a-d).

### Gene expression validation using the spatial transcriptomics analysis

The following four major cellular subgroups were identified through an unsupervised clustering analysis: VSMCs, T cells, macrophage, and ECs. These subgroups showed significantly different spatial distribution patterns (Figure 11a). Notably, the potential action

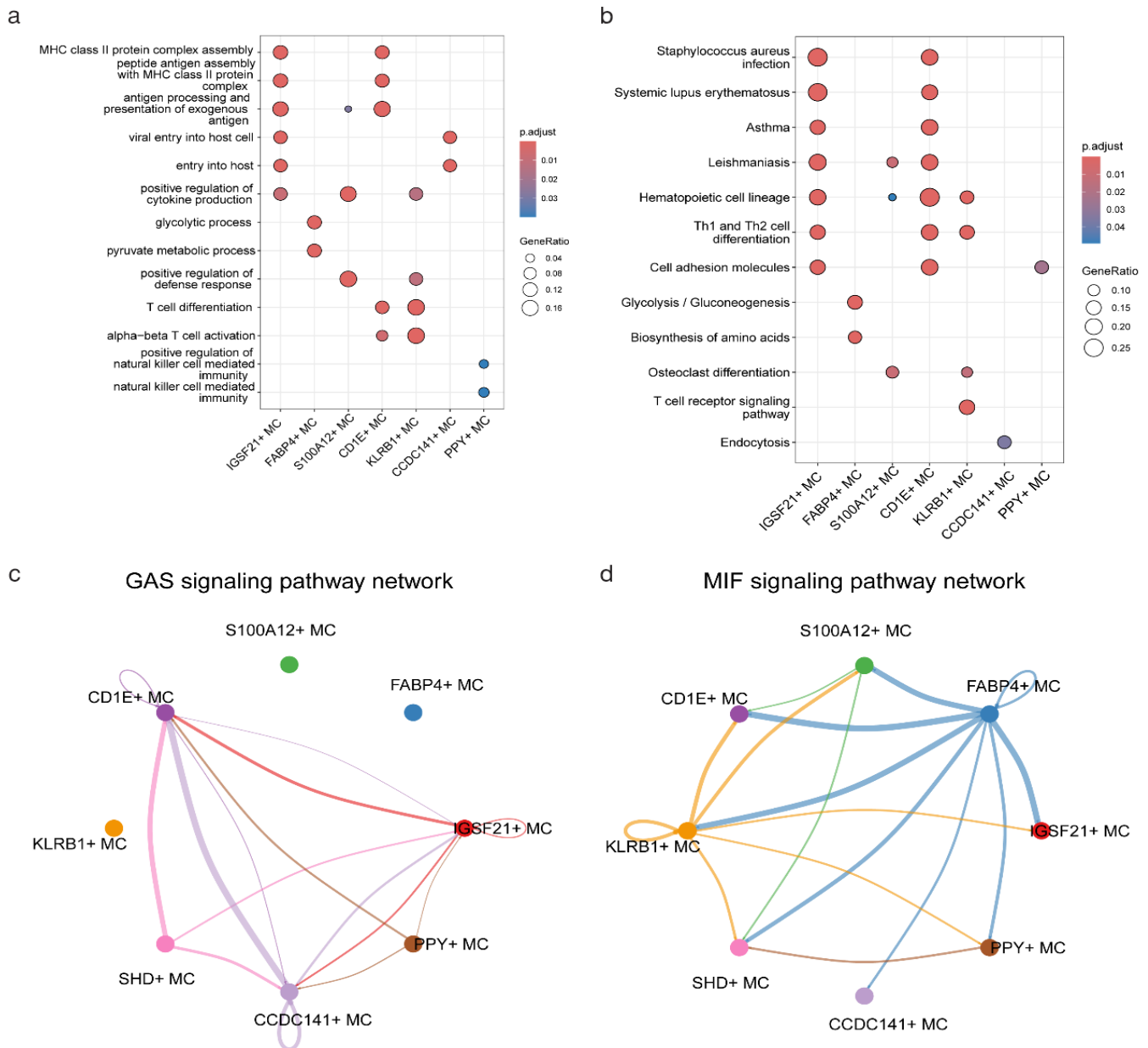


**FIG. 3.** Enrichment analysis and cell-cell communication of endothelial cells (EC). (a) The Gene Ontology enrichment analysis of EC subpopulations ( $n = 2634$  cells, adjusted  $p$ -value  $< 0.05$ , Benjamini-Hochberg method). (b) Different EC subpopulations communicate via the CXCL signaling pathway ( $p$ -value  $< 0.05$ ). (c) Different EC subpopulations communicate via the PTN signaling pathway ( $p$ -value  $< 0.05$ ).

KEGG, Kyoto Encyclopedia of Genes and Genomes; PTN, pleiotrophin.

targets of CBD screened by molecular docking, that is, *ACTC1*, *AKR1C2*, and *FABP4*, showed a specific expression in different plaque regions (Figures 11b-d).

DISCUSSION

Cardiovascular disease is the leading cause of death worldwide, with atherosclerosis being a chronic inflammatory condition constituting

the principal risk factor for its development. The current therapeutic strategies for atherosclerosis have rapidly advanced; however, they are accompanied by side effects and unable to cure the disease. Therefore, the novel drug and treatment strategy development has remained as an urgent need for atherosclerosis management.<sup>24</sup> In this study, we analyzed three distinct cell types, namely, MCs, ECs and VSMCs, to investigate the relevant signaling pathways within the cellular subpopulations and explore their intercellular crosstalk.

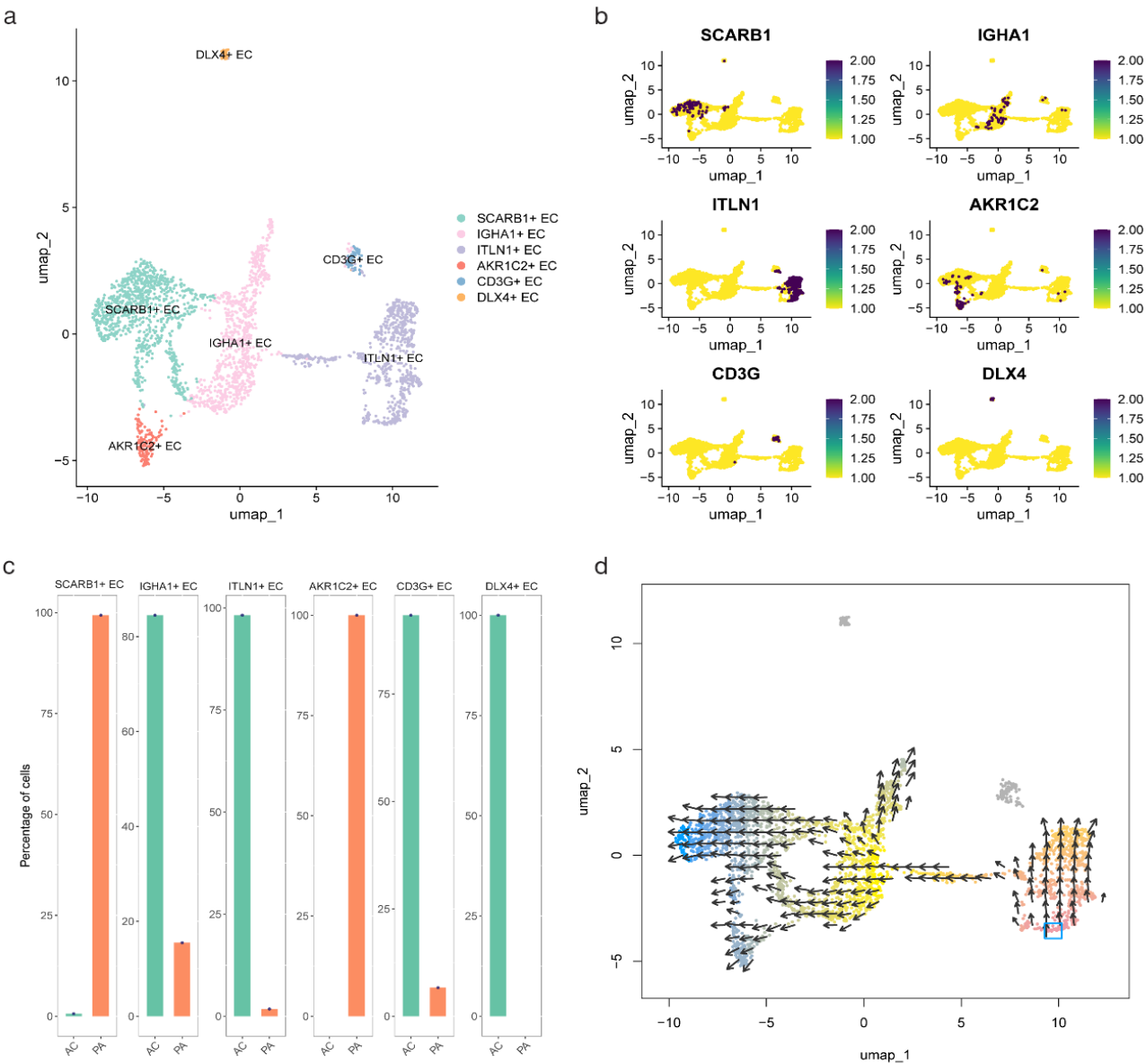


**FIG. 4.** Single-cell transcriptome analysis of endothelial cells (EC). (a) The UMAP plot illustrates the distribution of EC subpopulations, with distinct colors representing different EC subpopulations. (b) The density map illustrates the spatial density distribution of genes within EC subpopulations. The purple areas indicate higher cell density, while the yellow areas indicate lower cell density. (c) The bar chart illustrates the changes in the abundance of EC subpopulations between the atherosclerotic core group and the proximal artery group. (d) The VECTOR tool is used to infer the developmental direction of EC subpopulations.

UMAP, uniform manifold approximation and projection.

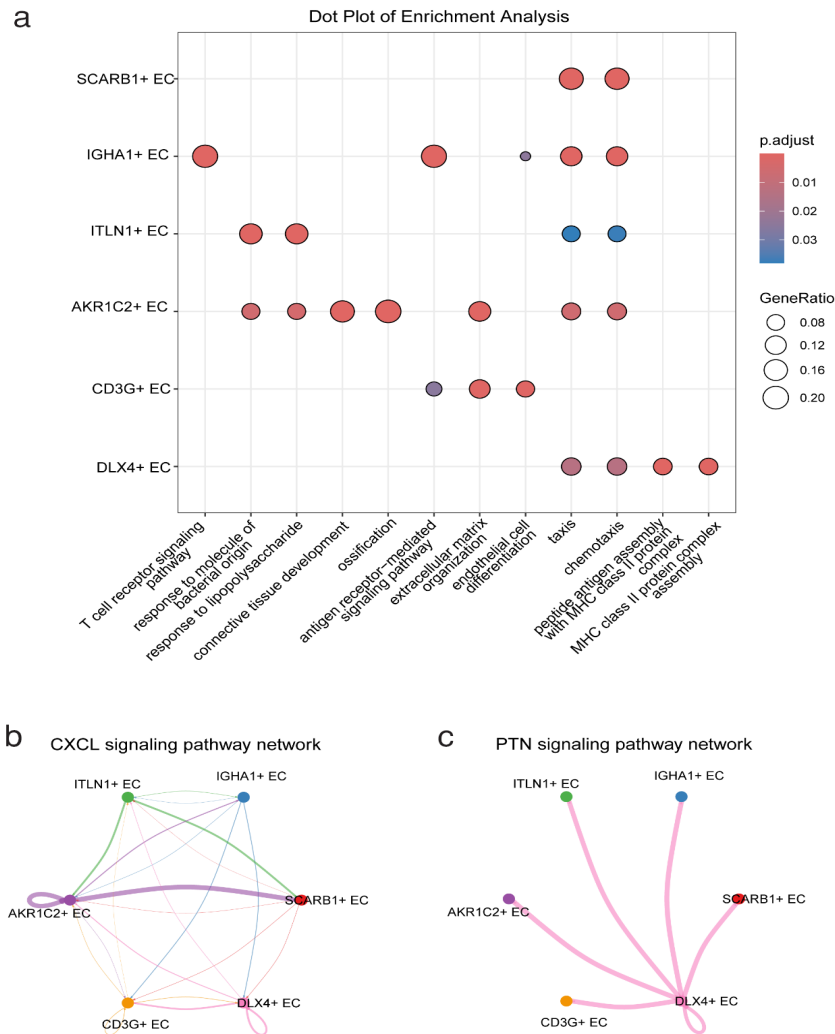


**FIG. 5.** Enrichment analysis and cell-cell communication of endothelial cells (EC). (a) The gene ontology enrichment analysis of EC subpopulations ( $n = 2634$  cells, adjusted  $p$ -value  $< 0.05$ , Benjamini-Hochberg method). (b) The KEGG enrichment analysis of EC subpopulations ( $n = 2634$  cells, adjusted  $p$ -value  $< 0.05$ , Benjamini-Hochberg method). (c) Different EC subpopulations communicate via the CXCL signaling pathway ( $p$ -value  $< 0.05$ ). (d) Different EC subpopulations communicate via the PTN signaling pathway ( $p$ -value  $< 0.05$ ).

KEGG, Kyoto Encyclopedia of Genes and Genomes; PTN, pleiotrophin.

We integrated single-cell transcriptomics, molecular docking, and spatial transcriptomics to introduce CBD into the CAS study and proposed a therapeutic strategy for CAS, thereby providing a theoretical basis for developing effective treatments.

Possessing anti-inflammatory and antioxidant properties and showing therapeutic potential in neurological disorders and cancer,<sup>25-28</sup> CBD improves metabolic syndrome by enhancing the homeostatic effects of the endocannabinoid system, thereby delaying the atherosclerosis onset and progression.<sup>29</sup> CBD and its methylated derivatives hold a significant therapeutic potential for atherosclerosis treatment.<sup>30</sup> Targeting the endocannabinoid signaling pathway, especially in macrophages, is a promising

strategy for combating atherosclerosis.<sup>31</sup> The endocannabinoid system modulates atherogenic dyslipidemia and atherosclerosis in both mice and humans.<sup>32</sup>

Fatty acid-binding protein 4 (*FABP4*), a protein primarily expressed in adipocytes and macrophages, plays a crucial role in lipid metabolism and immune responses.<sup>33</sup> The circulating *FABP4* levels are elevated under various pathological conditions, including atherosclerosis.<sup>34-37</sup> The *FABP4* levels are significantly associated with vulnerable plaque phenotypes, clinical symptoms, and the risk of adverse cardiovascular events.<sup>38-40</sup> Moreover, *FABP4*/aP2 modulates the macrophage redox signaling and inflammasome activation,<sup>41</sup> serving as a critical link between plaque instability and inflammation.<sup>42</sup> CBD



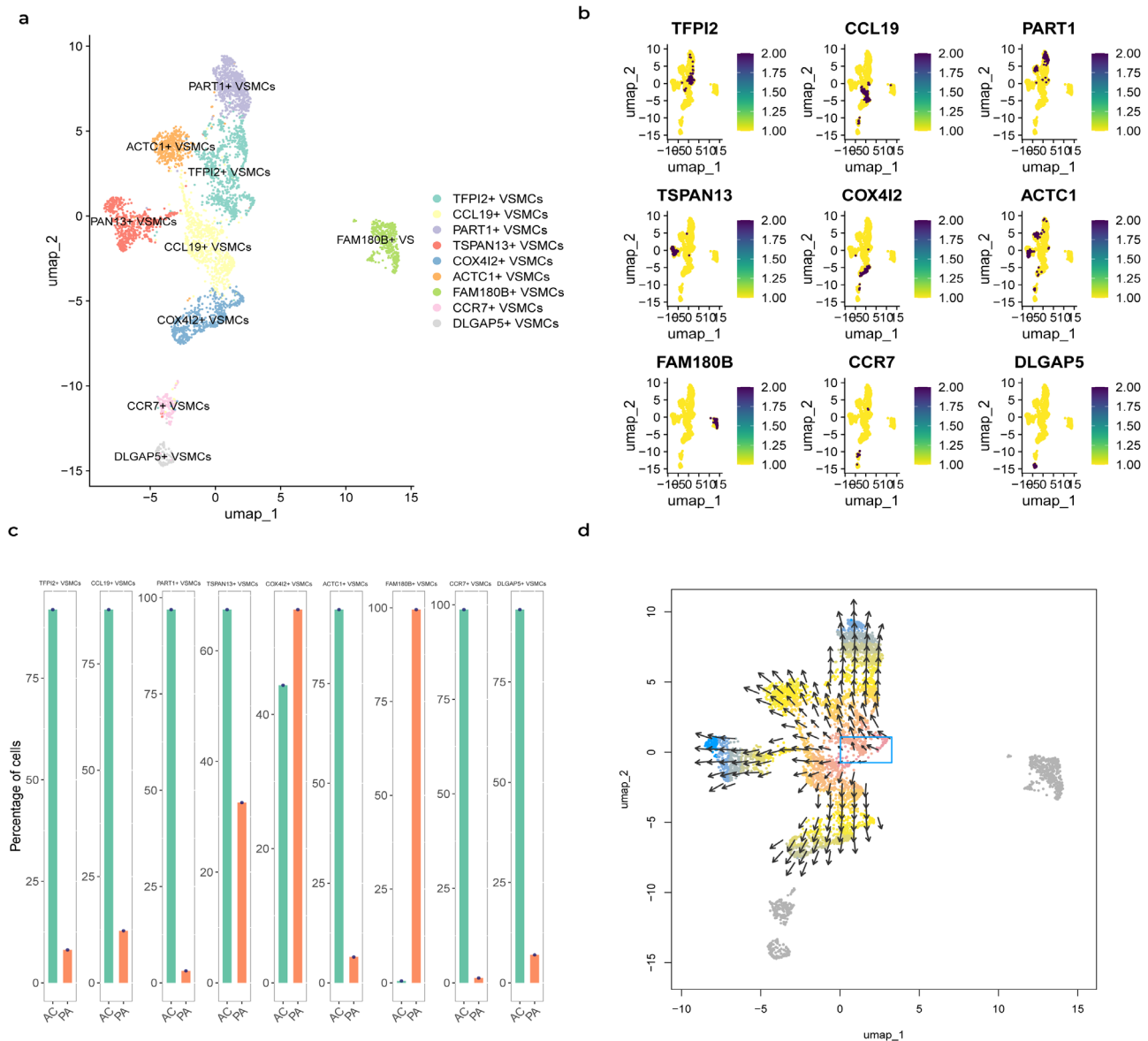


**FIG. 6.** Single-cell transcriptome analysis of vascular smooth muscle cells (VSMCs). (a) The UMAP plot illustrates the distribution of VSMCs subpopulations, with distinct colors representing different VSMCs subpopulations. (b) The density map illustrates the spatial density distribution of genes within VSMCs subpopulations. The purple areas indicate higher cell density, while the yellow areas indicate lower cell density. (c) The bar chart illustrates the changes in the abundance of VSMCs subpopulations between the atherosclerotic core (AC) group and the proximal artery (PA) group. (d) The VECTOR tool is used to infer the developmental direction of VSMCs subpopulations. UMAP, uniform manifold approximation and projection.

attenuates cytokine release and the nuclear factor (NF)- $\kappa$ B activity, thereby exhibiting context-dependent inflammatory responses under different inflammatory conditions.<sup>43,44</sup>

*S100A12* is a pro-inflammatory protein secreted by neutrophils; studies show that it is associated with vascular inflammation and atherosclerosis.<sup>45</sup> Elevated serum *S100A12* levels are associated with a poor prognosis in cardiovascular diseases, consequently making

it a potential therapeutic target.<sup>46,47</sup> *S100A12* plays an important role in vascular calcification, inflammation, and oxidative stress.<sup>48</sup> *S100A12* is expressed by neutrophils and monocytes/macrophages, activates intracellular signaling pathways like the NF- $\kappa$ B pathway, and induces pro-inflammatory responses, making it a valuable biomarker under inflammatory conditions.<sup>49</sup> Moreover, *S100A12* is associated with plaque instability and linked to atherosclerosis development.<sup>50</sup>

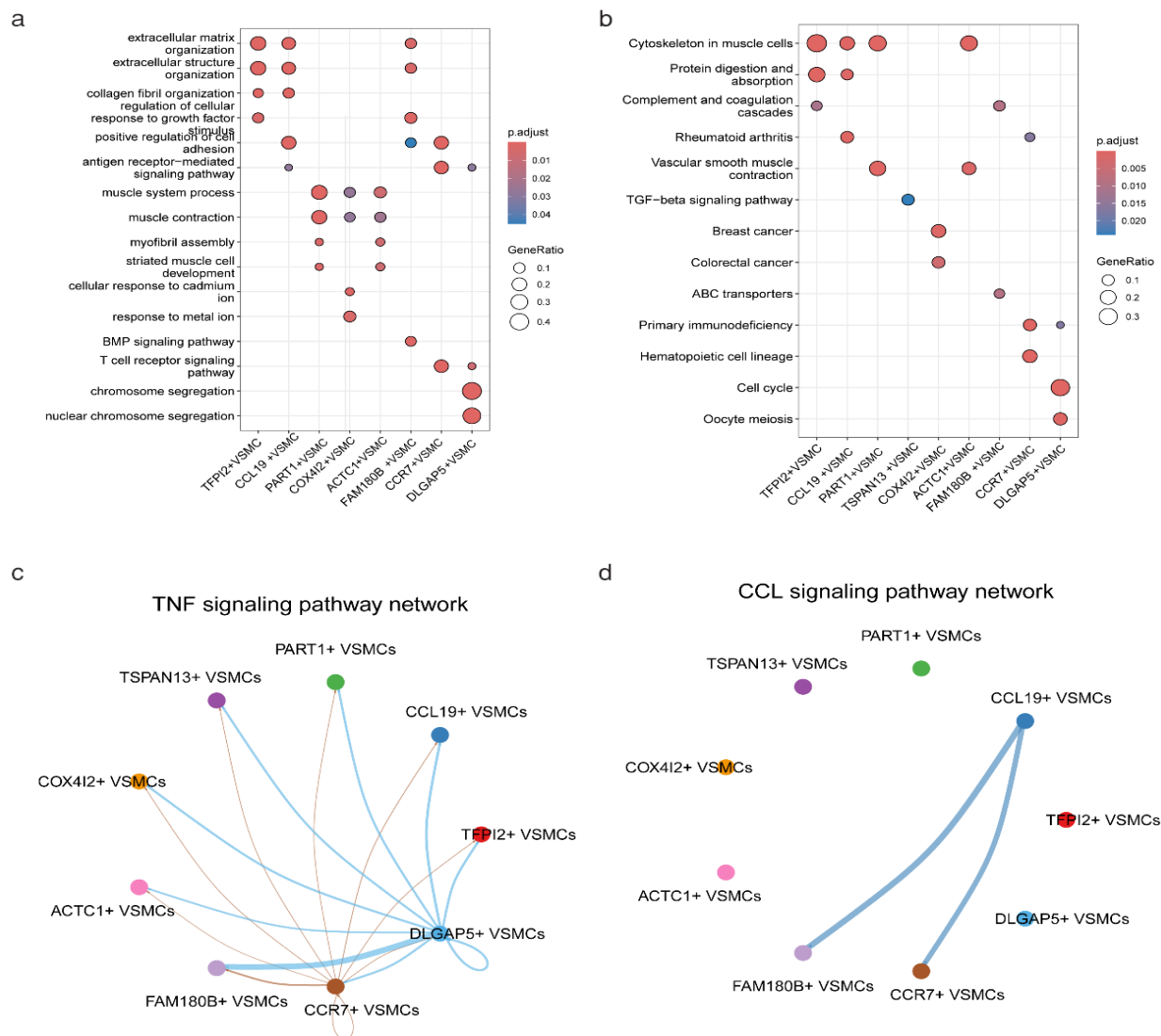


**FIG. 7.** Enrichment analysis and cell-cell communication of vascular smooth muscle cells (VSMCs). (a) The gene ontology enrichment analysis of VSMCs subpopulations ( $n = 4424$  cells, adjusted  $p$ -value  $< 0.05$ , Benjamini-Hochberg method). (b) The KEGG enrichment analysis of VSMCs subpopulations ( $n = 4424$  cells, adjusted  $p$ -value  $< 0.05$ , Benjamini-Hochberg method). (c) Different VSMCs subpopulations communicate via the TNF signaling pathway ( $p$ -value  $< 0.05$ ). (d) Different VSMCs subpopulations communicate via the CCL signaling pathway ( $p$ -value  $< 0.05$ ).

KEGG, Kyoto Encyclopedia of Genes and Genomes; TNF, tumor necrosis factor.

The CellChat analysis revealed that the GAS, MIF, CXCL, and PTN signaling pathways mediate the intercellular interactions among the different cell subpopulations in CAS. The vitamin K-dependent protein, Gas6, promotes the SMC survival and migration and activates the ECs and leukocytes, thereby contributing to atherogenesis. MIF is markedly upregulated in vulnerable plaques, weakens the fibrous cap, and drives plaque destabilization.<sup>51,52</sup> Meanwhile, CXCL16 functions as a chemokine, an adhesion molecule, and a scavenger receptor and is involved in the formation of carotid atherosclerotic plaques.<sup>53,54</sup> PTN is expressed in the atherosclerosis-prone coronary arteries where it colocalizes with the microvessels, and its expression

is regulated by the IFN- $\gamma$ /JAK/STAT1 signaling pathway.<sup>55</sup> In carotid atherosclerosis, CCL19 and CCL21 are upregulated: CCL21 accelerates the lipid accumulation in the macrophages, while CCL19 stimulates a VSMC proliferation, together with driving atherogenesis.<sup>56</sup> Compared with stable plaques, vulnerable ones exhibit elevated CCL14 and VEGF-A expressions. CCL14 upregulates VEGF-A by activating the JAK2/STAT3 pathway, consequently inducing neovascularization and driving the plaque progression toward vulnerability.<sup>57</sup> In ruptured human atherosclerotic plaques, CCL18 is markedly upregulated and predominantly enriched in the macrophages. The CCL18/CCR6 axis serves as a key regulator of the immune response in atherosclerosis.<sup>58</sup>

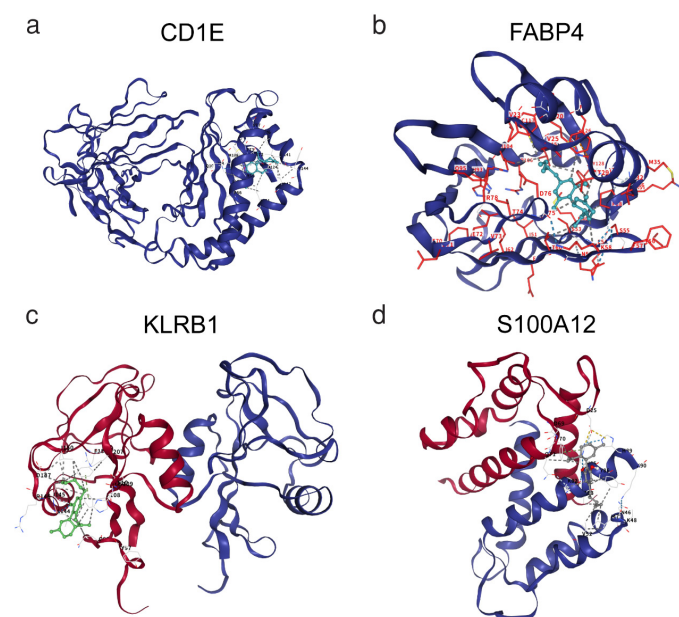


**FIG. 8.** Molecular docking of cannabidiol to protein targets of macrophage marker genes. (a) *CD1E*; (b) *FABP4*; (c) *KLRB1*; (d) *S100A12*.

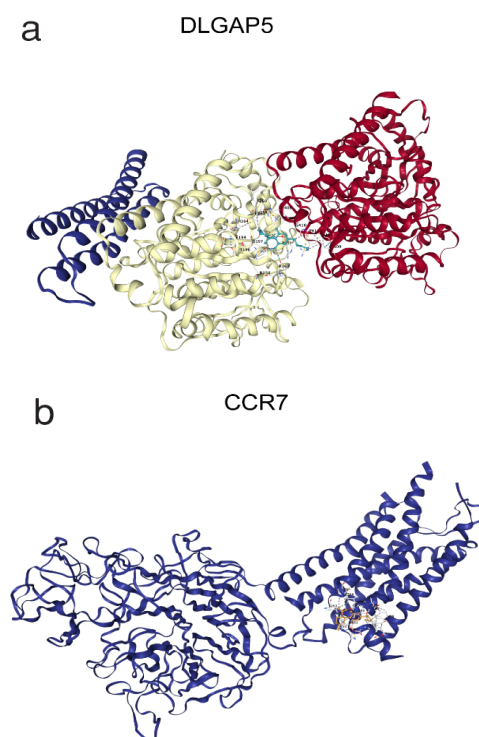


**FIG. 10.** Molecular docking of cannabidiol to protein targets of vascular smooth muscle cells marker genes. (a) *DLGAP5*; (b) *CCR7*.

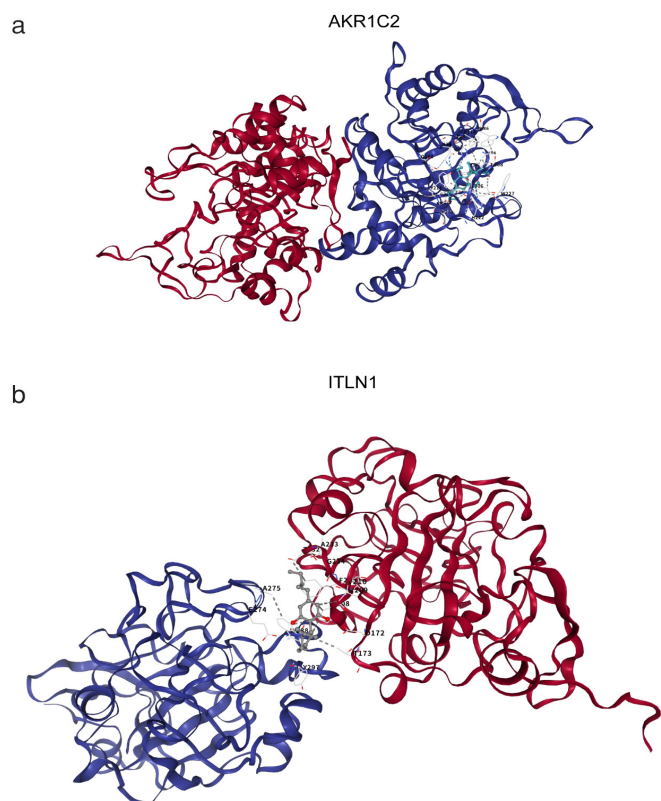


**FIG. 9.** Molecular docking of cannabidiol to protein targets of endothelial cells marker genes. (a) *AKR1C2*; (b) *ITLN1*.

In summary, through an in-depth analysis of the functional characteristics of specific cellular subpopulations and the regulatory mechanisms of their associated signaling pathways, this study has fully revealed the key roles of cellular subpopulations in the pathological process of CAS. Our research provides a new perspective for a deeper understanding of the molecular mechanisms of CAS and confirms the potential of CBD in CAS treatment. This work provides a theoretical basis for the future development of CAS treatment strategies.

By elucidating the roles of specific cellular subpopulations in CAS and their modulation of the relevant signaling pathways, this work highlights their critical functions in this disease and provides new insights into the molecular mechanism of CAS by integrating single-cell transcriptomics, molecular docking, and spatial transcriptomics. This study also provides a theoretical reference for the future development of treatment strategies against CAS.

Our work has limitations. The expression levels of *FABP4*, *S100A12*, *AKR1C2*, and *ACTC1* and the TNF-, CXCL-, and MIF-signaling pathways are not experimentally validated, thereby requiring further verification. The positive docking results for *ACTC1* and *DLGAP5* must be regarded merely as hypotheses at the pure computational level, thus still requiring an experimental validation in the future.

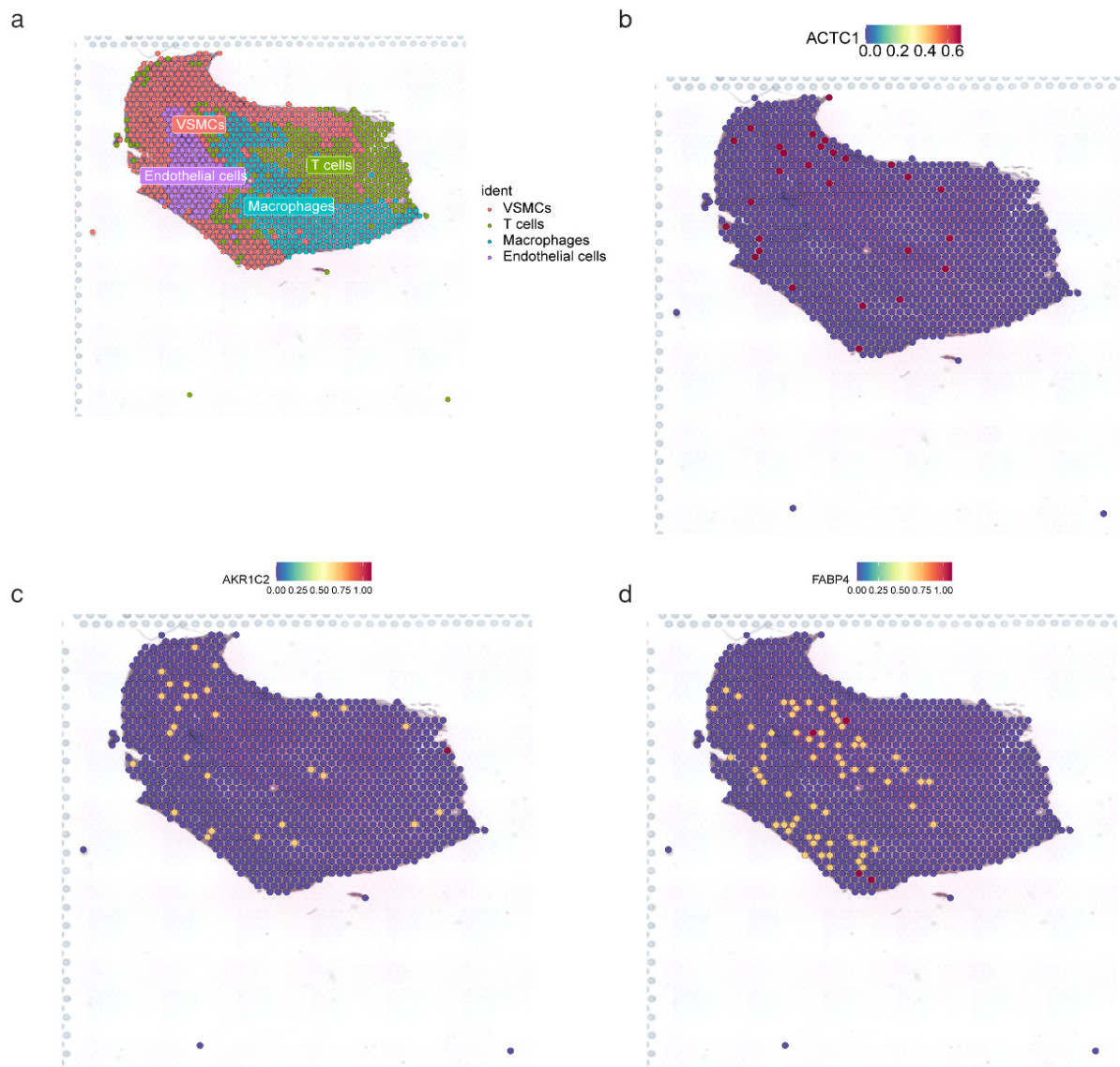


**FIG. 11.** Spatial transcriptomics reveal gene expression patterns in carotid atherosclerotic plaques. (a) Spatial transcriptomic cell annotation of carotid atherosclerotic plaques; (b) Spatial expression pattern of *ACTC1* in carotid atherosclerotic plaques; (c) Spatial expression profile of *AKR1C2* in carotid atherosclerotic plaques; (d) Spatial distribution of *FABP4* expression in carotid atherosclerotic plaques.

Although existing studies show that *ACTC1* is associated with the immune microenvironment formation in CAS plaques,<sup>59</sup> no currently published evidence links *DLGAP5* to CAS. All the scRNA-seq analyses were conducted solely on the single dataset, GSE159677, without external datasets or validation in an independent cohort. The future work must expand both scRNA-seq and spatial transcriptomic datasets to capture the spatial heterogeneity and the inter-

individual variability. Our sample size was limited. Although the molecular docking data support CBD's binding to the target protein, experimental validation must be done to clarify its mechanism of action. Translational studies must prioritize the evaluation of CBD's therapeutic efficacy in established CAS animal models, followed by early-phase clinical trials in patients with CAS to systematically assess its safety and effects on relevant biomarkers.



**Ethics Committee Approval:** The data for this study were obtained from public databases and no additional ethical approval was required.

**Informed Consent:** Not applicable.

**Data Sharing Statement:** The datasets analyzed during the current study are available from the corresponding author upon reasonable request.

**Authorship Contributions:** Concept- R.Q., H.X., L.C.; Design- R.Q., H.X., L.C.; Supervision- L.C.; Materials- R.Q.; Data Collection or Processing- R.Q., H.X.; Analysis and/or Interpretation- R.Q., H.X., Q.Q.; Literature Review- R.Q., H.X., Q.Q., W.X., X.L., L.C.; Writing- R.Q., H.X., Q.Q., W.X., X.L., L.C.; Critical Review- R.Q., H.X., Q.Q., W.X., X.L., L.C.

**Conflict of Interest:** The authors declare that they have no conflict of interest.

**Funding:** This study was supported by grants from the National Natural Science Foundation of China (82271371 and 82260367), the High-Level Medical Expert Training Program of Guangxi "139" Plan Funding, the Guangxi Medical and Health Appropriate Technology Development and Application Project (S2021107), the Clinical Research "Climbing" Program of the First Affiliated Hospital of Guangxi Medical University (YYZS2021002), the Advanced Innovation Teams and Xinghu Scholars Program of Guangxi Medical University.

**Supplementary Table 1.** <https://balkanmedicaljournal.org/img/files/BalkanMedJ-2025-8-151.pdf>

## REFERENCES

- Dossabhoys S, Arya S. Epidemiology of atherosclerotic carotid artery disease. *Semin Vasc Surg.* 2021;34:3-9. [\[CrossRef\]](#)
- Xing L, Li R, Zhang S, et al. High burden of carotid atherosclerosis in rural Northeast China: a population-based study. *Front Neurol.* 2021;12:597992. [\[CrossRef\]](#)
- Brook RD, Bard RL, Patel S, et al. A negative carotid plaque area test is superior to other noninvasive atherosclerosis studies for reducing the likelihood of having underlying significant coronary artery disease. *Arterioscler Thromb Vasc Biol.* 2006;26:656-662. [\[CrossRef\]](#)
- Prabhakaran S, Rundek T, Ramas R, et al. Carotid plaque surface irregularity predicts ischemic stroke: the northern Manhattan study. *Stroke.* 2006;37:2696-2701. [\[CrossRef\]](#)
- Rubin MR, Rundek T, McMahon DJ, Lee HS, Sacco RL, Silverberg SJ. Carotid artery plaque thickness is associated with increased serum calcium levels: the Northern Manhattan study. *Atherosclerosis.* 2007;194:426-432. [\[CrossRef\]](#)
- Mathiesen EB, Johnsen SH. Ultrasonographic measurements of subclinical carotid atherosclerosis in prediction of ischemic stroke. *Acta Neurol Scand Suppl.* 2009;(189):68-72. [\[CrossRef\]](#)
- Rassi CH, Churchill TW, Tavares CA, et al. Use of imaging and clinical data to screen for cardiovascular disease in asymptomatic diabetics. *Cardiovasc Diabetol.* 2016;15:28. [\[CrossRef\]](#)
- Rundek T, Arif H, Boden-Albala B, Elkind MS, Paik MC, Sacco RL. Carotid plaque, a subclinical precursor of vascular events: the Northern Manhattan Study. *Neurology.* 2008;70:1200-1207. [\[CrossRef\]](#)
- Hajkarim MC, Won KJ. Single Cell RNA-Sequencing for the study of atherosclerosis. *J Lipid Atheroscler.* 2019;8:152-161. [\[CrossRef\]](#)
- Fernandez DM, Rahman AH, Fernandez NF, et al. Single-cell immune landscape of human atherosclerotic plaques. *Nat Med.* 2019;25:1576-1588. [\[CrossRef\]](#)
- Depuydt MAC, Prange KHM, Slenders L, et al. Microanatomy of the human atherosclerotic plaque by single-cell transcriptomics. *Circ Res.* 2020;127:1437-1455. [\[CrossRef\]](#)
- H Härdtner C, Remmersmann F, Ehlert C, et al. NLRP3 mediates lipid-driven macrophage proliferation in established atherosclerosis. *Basic Res Cardiol.* 2025. [\[CrossRef\]](#)
- Chen PY, Qin L, Baeyens N, et al. Endothelial-to-mesenchymal transition drives atherosclerosis progression. *J Clin Invest.* 2015;125:4514-4528. [\[CrossRef\]](#)
- Evrard SM, Lecce L, Michelis KC, et al. Endothelial to mesenchymal transition is common in atherosclerotic lesions and is associated with plaque instability. Erratum in: *Nat Commun.* 2019;8:14710. [\[CrossRef\]](#)
- Gomez D, Owens GK. Smooth muscle cell phenotypic switching in atherosclerosis. *Cardiovasc Res.* 2012;95:156-164. [\[CrossRef\]](#)
- Alencar GF, Owsiany KM, Karnewar S, et al. Stem cell pluripotency genes Klf4 and Oct4 regulate complex SMC phenotypic changes critical in late-stage atherosclerotic lesion pathogenesis. *Circulation.* 2020;142:2045-2059. [\[CrossRef\]](#)
- Guo Y, Wei R, Deng J, Guo W. Research progress in the management of vascular disease with cannabidiol: a review. *J Cardiothorac Surg.* 2024;19:6. [\[CrossRef\]](#)
- Rajesh M, Mukhopadhyay P, Bátkai S, et al. Cannabidiol attenuates high glucose-induced endothelial cell inflammatory response and barrier disruption. *Am J Physiol Heart Circ Physiol.* 2007;293:H610-9. [\[CrossRef\]](#)
- He M, Shi J, Xu YJ, Liu Y. Cannabidiol (CBD) inhibits foam cell formation via regulating cholesterol homeostasis and lipid metabolism. *Mol Nutr Food Res.* 2024;68:e2400154. [\[CrossRef\]](#)
- Wu T, Hu E, Xu S, et al. clusterProfiler 4.0: a universal enrichment tool for interpreting omics data. *Innovation (Camb).* 2021;2:100141. [\[CrossRef\]](#)
- Zhang F, Li X, Tian W. Unsupervised inference of developmental directions for single cells using VECTOR. *Cell Rep.* 2020;32:108069. [\[CrossRef\]](#)
- Alsaigh T, Evans D, Frankel D, Torkamani A. Decoding the transcriptome of calcified atherosclerotic plaque at single-cell resolution. *Commun Biol.* 2022;5:1084. [\[CrossRef\]](#)
- Singla S, Sachdeva R, Mehta JL. Cannabinoids and atherosclerotic coronary heart disease. *Clin Cardiol.* 2012;35:329-335. [\[CrossRef\]](#)
- Wang Z, He X, Bai H, et al. Recent progress in anti-atherosclerosis strategies and prospective therapeutic targets. *Int J Pharm.* 2025;684:126122. [\[CrossRef\]](#)
- Pisanti S, Malfitano AM, Ciaglia E, et al. Cannabidiol: state of the art and new challenges for therapeutic applications. *Pharmacol Ther.* 2017;175:133-150. [\[CrossRef\]](#)
- Atalay S, Jarocka-Karpowicz I, Skrzydlewska E. Antioxidative and anti-inflammatory properties of cannabidiol. *Antioxidants (Basel).* 2019;9:21. [\[CrossRef\]](#)
- Kis B, Ifrim FC, Buda V, et al. Cannabidiol-from plant to human body: a promising bioactive molecule with multi-target effects in cancer. *Int J Mol Sci.* 2019;20:5905. [\[CrossRef\]](#)
- Martínez V, Iriando De-Hond A, Borrelli F, Capasso R, Del Castillo MD, Abalo R. Cannabidiol and other non-psychoactive cannabinoids for prevention and treatment of gastrointestinal disorders: useful nutraceuticals? *Int J Mol Sci.* 2020;21:3067. [\[CrossRef\]](#)
- Scharf EL. Translating Endocannabinoid biology into clinical practice: cannabidiol for stroke prevention. *Cannabis Cannabinoid Res.* 2017;2:259-264. [\[CrossRef\]](#)
- Takeda S, Usami N, Yamamoto I, Watanabe K. Cannabidiol-2',6'-dimethyl ether, a cannabidiol derivative, is a highly potent and selective 15-lipoxygenase inhibitor. *Drug Metab Dispos.* 2009;37:1733-1737. [\[CrossRef\]](#)
- Immenschuh S. Endocannabinoid signalling as an anti-inflammatory therapeutic target in atherosclerosis: does it work? *Cardiovasc Res.* 2009;84:341-342. [\[CrossRef\]](#)
- Guo Y, Wei X, Pei J, Yang H, Zheng XL. Dissecting the role of cannabinoids in vascular health and disease. *J Cell Physiol.* 2024;239:e31373. [\[CrossRef\]](#)
- Hu Z, Liu W, Hua X, et al. Single-cell transcriptomic atlas of different human cardiac arteries identifies cell types associated with vascular physiology. *Arterioscler Thromb Vasc Biol.* 2021;41:1408-1427. [\[CrossRef\]](#)
- Cabré A, Lázaro I, Girona J, et al. Plasma fatty acid binding protein 4 is associated with atherogenic dyslipidemia in diabetes. *J Lipid Res.* 2008;49:1746-1751. [\[CrossRef\]](#)
- Furuhashi M, Fuseya T, Murata M, et al. Local production of fatty acid-binding protein 4 in epicardial/perivascular fat and macrophages is linked to coronary atherosclerosis. *Arterioscler Thromb Vasc Biol.* 2016;36:825-834. [\[CrossRef\]](#)
- Furuhashi M, Hotamisligil GS. Fatty acid-binding proteins: role in metabolic diseases and potential as drug targets. *Nat Rev Drug Discov.* 2008;7:489-503. [\[CrossRef\]](#)
- Furuhashi M, Saitoh S, Shimamoto K, Miura T. Fatty acid-binding protein 4 (FABP4): pathophysiological insights and potential clinical biomarker of metabolic and cardiovascular diseases. *Clin Med Insights Cardiol.* 2015;8:23-33. [\[CrossRef\]](#)
- Lee K, Santibanez-Koref M, Polvikoski T, Birchall D, Mendelow AD, Keavney B. Increased expression of fatty acid binding protein 4 and leptin in resident macrophages characterises atherosclerotic plaque rupture. *Atherosclerosis.* 2013;226:74-81. [\[CrossRef\]](#)
- Pugliese G, Iacobini C, Blasetti Fantauzzi C, Menini S. The dark and bright side of atherosclerotic calcification. *Atherosclerosis.* 2015;238:220-230. [\[CrossRef\]](#)
- Y Yap C, Mieremet A, de Vries CJM, Micha D, de Waard V. Six shades of vascular smooth muscle cells illuminated by KLF4 (Krüppel-Like Factor 4). *Arterioscler Thromb Vasc Biol.* 2021;41:2693-2707. [\[CrossRef\]](#)

41. Steen KA, Xu H, Bernlohr DA. FABP4/aP2 regulates macrophage redox signaling and inflammasome activation via control of UCP2. *Mol Cell Biol*. 2017;37:e00282-16. [\[CrossRef\]](#)
42. Agardh HE, Folkersen L, Ekstrand J, et al. Expression of fatty acid-binding protein 4/aP2 is correlated with plaque instability in carotid atherosclerosis. *J Intern Med*. 2011;269:200-210. [\[CrossRef\]](#)
43. Muthumalage T, Rahman I. Cannabidiol differentially regulates basal and LPS-induced inflammatory responses in macrophages, lung epithelial cells, and fibroblasts. *Toxicol Appl Pharmacol*. 2019;382:114713. [\[CrossRef\]](#)
44. Confidentiality and societal obligation. Summary of discussion results. *Prog Clin Biol Res*. 1980;38:253-255. [\[CrossRef\]](#)
45. Zhang Q, Ding X, Xu Y, Lin Y, Wu Y. Neutrophil-mediated effects of S100A12 on major adverse cardiovascular events: insights from the UK biobank. *Am J Prev Cardiol*. 2025;23:101278. [\[CrossRef\]](#)
46. Saito T, Hojo Y, Ogoyama Y, et al. S100A12 as a marker to predict cardiovascular events in patients with chronic coronary artery disease. *Circ J*. 2012;76:2647-52. [\[CrossRef\]](#)
47. Grauen Larsen H, Yndigegn T, Marinkovic G, et al. The soluble receptor for advanced glycation end-products (sRAGE) has a dual phase-dependent association with residual cardiovascular risk after an acute coronary event. *Atherosclerosis*. 2019;287:16-23. [\[CrossRef\]](#)
48. Xiao X, Yang C, Qu SL, et al. S100 proteins in atherosclerosis. *Clin Chim Acta*. 2020;502:293-304. [\[CrossRef\]](#)
49. Nazari A, Khorramdelazad H, Hassanshahi G, et al. S100A12 in renal and cardiovascular diseases. *Life Sci*. 2017;191:253-258. [\[CrossRef\]](#)
50. Abbas A, Aukrust P, Dahl TB, et al. High levels of S100A12 are associated with recent plaque symptomatology in patients with carotid atherosclerosis. Erratum in: *Stroke*. 2013;44:e82. [\[CrossRef\]](#)
51. Clauser S, Meilhac O, Bièche I, et al. Increased secretion of Gas6 by smooth muscle cells in human atherosclerotic carotid plaques. *Thromb Haemost*. 2012;107:140-149. [\[CrossRef\]](#)
52. Kong YZ, Huang XR, Ouyang X, et al. Evidence for vascular macrophage migration inhibitory factor in destabilization of human atherosclerotic plaques. *Cardiovasc Res*. 2005;65:272-282. [\[CrossRef\]](#)
53. Lv Y, Hou X, Ti Y, Bu P. Associations of CXCL16/CXCR6 with carotid atherosclerosis in patients with metabolic syndrome. *Clin Nutr*. 2013;32:849-854. [\[CrossRef\]](#)
54. Canton J, Neculai D, Grinstein S. Scavenger receptors in homeostasis and immunity. *Nat Rev Immunol*. 2013;13:621-634. [\[CrossRef\]](#)
55. Li F, Tian F, Wang L, Williamson IK, Sharifi BG, Shah PK. Pleiotrophin (PTN) is expressed in vascularized human atherosclerotic plaques: IFN- $\gamma$ /JAK/STAT1 signaling is critical for the expression of PTN in macrophages. *FASEB J*. 2010;24:810-822. [\[CrossRef\]](#)
56. Halvorsen B, Dahl TB, Smedbakken LM, et al. Increased levels of CCR7 ligands in carotid atherosclerosis: different effects in macrophages and smooth muscle cells. *Cardiovasc Res*. 2014;102:148-156. [\[CrossRef\]](#)
57. Li Z, Qin Z, Kong X, et al. CCL14 exacerbates intraplaque vulnerability by promoting neovascularization in the human carotid plaque. *J Stroke Cerebrovasc Dis*. 2022;31:106670. [\[CrossRef\]](#)
58. Singh A, Kraaijeveld AO, Curaj A, et al. CCL18 aggravates atherosclerosis by inducing CCR6-dependent T-cell influx and polarization. *Front Immunol*. 2024;15:1327051. [\[CrossRef\]](#)
59. Zhang Y, Zhang L, Jia Y, Fang J, Zhang S, Hou X. Screening of potential regulatory genes in carotid atherosclerosis vascular immune microenvironment. *PLoS One*. 2024;19:e0307904. [\[CrossRef\]](#)